Available online at www.sciencedirect.com
SCIENCE DIRECT
Polymer 46 (2005) 3149–3156
polymer
www.elsevier.com/locate/polymer

Photo-oxidative degradation of polypropylene/montmorillonite nanocomposites

Huaili Qin[a,c], Shimin Zhang[a,*], Huiju Liu[a], Shaobo Xie[a,c], Mingshu Yang[a,*], Deyan Shen[b]

[a]*CAS Key Laboratory of Engineering Plastics, Joint Laboratory of Polymer Science and Materials, Institute of Chemistry, Chinese Academy of Sciences, Beijing 100080, People's Republic of China*

[b]*State Key Laboratory of Polymer Physics and Chemistry, Joint Laboratory of Polymer Science and Materials, Institute of Chemistry, Chinese Academy of Sciences, Beijing 100080, People's Republic of China*

[c]*Graduate school, Chinese Academy of Sciences, Beijing 100039, People's Republic of China*

Received 15 October 2004; received in revised form 24 January 2005; accepted 29 January 2005
Available online 10 March 2005

Abstract

The photo-oxidative behavior of the polypropylene (PP)/montmorillonite (MMT) nanocomposites and microcomposites has been investigated upon ultraviolet exposure using the technique of infrared spectroscopy. The rate of photo-oxidative degradation of PP/MMT nanocomposites is much faster than that of pure PP. The influence of pristine MMT, alkylammonium and compatibilizer were investigated, respectively. All these components can catalyze the photo-oxidation of PP matrix, in which the influence of compatibilizer and pristine MMT is primary. Moreover, the dispersion state of the clay particles in the polymer matrices has a little influence on the photo-oxidative degradation of polymer matrix. Consequently, an integrated catalysis mechanism of the photo-oxidative degradation of PP clay nanocomposite is proposed. It would provide benefit direction for the preparation and usage of polymer layered silicate nanocomposites (PLSN).

Keywords: Polypropylene; Montmorillonite; Photo-oxidative degradation

1. Introduction

Environmental durability is a key feature for polymer–clay nanocomposites in their processing and usage due to their degradation. There are many factors influencing the degradation of polymeric materials, such as photo-irradiation, thermo-degradation, oxidation, hydrolization etc., and the combinations. Within the various factors, the photo-oxidation plays an important role. Thus, the study on photo-oxidative degradation of polymeric materials is always attracting attention in the field of polymer degradation and stability.

In the past decade, polymer layered silicate nanocomposites (PLSN) have received great attention whether in fundamental research or industry exploitation and have been considered as a new-generation of composite materials [1–4]. Compared to the conventional filled polymers, PLSN have many unique properties in the presence of a small amount of the silicate, such as enhanced mechanical properties, increased heat distortion temperature, improved thermal stability, decreased gas/vapor permeability and reduced flammability [5–11].

The typical natural mineral in the smectite clay, montmorillonite (MMT), is the most commonly used, which belongs to the general family of 2:1 layered silicates. The layer structure of MMT consists of two silica tetrahedral sheets to an edge-shared octahedral sheet of either aluminum or magnesium hydroxide. Stacking of the layers of around 1 nm thickness by a weak dipolar force leads to interlayers or galleries between the layers. The galleries are normally occupied by cations such as Na^+, K^+, Ca^{2+} and Mg^{2+}, by which is easily organified by ion-exchange reaction with alkylammonium cations [12]. The modified clay (organoclay) becomes organophilic, its surface energy is lower and is more compatible with organic polymers. Under well-defined experimental conditions,

* Corresponding author. Tel.: +86 10 82615665; fax: +86 10 62559373.
E-mail addresses: smzhang@iccas.ac.cn (S. Zhang), yms@iccas.ac.cn (M. Yang).

0032-3861/$ - see front matter © 2005 Elsevier Ltd. All rights reserved.
doi:10.1016/j.polymer.2005.01.087

these polymers may be able to intercalate within the galleries, leading to an intercalated or exfoliated structure. As the research progressed in this field, a series of PLSN has been developed and some of them have been found application in automotive and electric industry.

There are some works in the literature concerning the photo-oxidative degradation of PLSN. In our previous work, the photo-aging behaviors of polyethylene/montmorillonite (PE/MMT) [13,14] and polyamide 6/montmorillonite (PA6/MMT) [15] nanocomposites have been investigated. The rate of photo-oxidative degradation of PE/MMT nanocomposite is much faster than that of pure PE. The acceleration of photo-oxidation of PE/MMT nanocomposite is due to the nature of MMT and interlayer ammonium ions, in which the influence of interlayer ammonium ions is primary [13]. Through the study of influence of interlayer cations in MMT, an integrated catalysis mechanism of the photo-oxidative degradation of PE/MMT nanocomposites is proposed [14]. The decomposition of ammonium ion may create acidic sites on layered silicates; meanwhile the complex crystallographic structure and habit of clay minerals could also result in some active sites. All these active sites can induce the formation of free radical upon UV irradiation and accelerate the photo-oxidative degradation of PE matrix. Wilkie et al. [16] reported that the photo-oxidative degradation of polypropylene/montmorillonite (PP/MMT) nanocomposites is faster than that of pure polypropylene. They suspected that the acceleration was caused by clay or the structure form of the nanocomposites. Gardette et al. [17] reported a study on the influence of organoclay and compatibilizer on photo-oxidation of PP/MMT nanocomposites. However, the influence of each component and clay dispersion state on the photo-oxidation of the PP/MMT nanocomposites is still not clear.

Polypropylene (PP) is one of the most widely used polyolefin polymers. Due to the quasi-apolar nature of PP, large quantity of compatibilizers containing polar groups, such as maleic anhydride-grafted-polypropylene copolymers, are generally introduced as the third component to compensate the difference of polarity between the resin matrix and the nanoscale fillers during the preparation of PP/MMT nanocomposites [18–21]. In order to understand the influence of each components and clay dispersion state on photo-oxidation mechanism of PLSN, we describe the photo-oxidation behavior of polypropylene/montmorillonite (PP/MMT) composites in this paper. It is shown that the rate of photo-oxidative degradation of PP/MMT nanocomposite is much fast than that of pure PP. The influence of pristine MMT, alkylammonium and compatibilizer were investigated, respectively. The experiment results indicate that all these components can accelerate the photo-oxidation of PP matrix. The influence of dispersion state of MMT in polymer matrix has also been discussed.

2. Experimental

2.1. Materials

The isotactic polypropylene, 1300, was purchased from Yanshan Petrochemical Co Ltd, Beijing, China. The maleic anhydride-grafted-polypropylene copolymer (MI 30 g/10 min, amount of MA 0.8%, termed PP-g-MA) was purchased from Shanghai Genius Advanced Material Co. Ltd, Shanghai, China. Dioctadecyldimethyl ammonium chloride [$(C_{18}H_{37})_2N^+(CH_3)_2Cl^-$, denoted with 2C18], octadecyltrimethyl ammonium chloride [$C_{18}H_{37}N^+(CH_3)_3Cl^-$, denoted with C18] and ammonium chloride (NH_4Cl) were purchased from Beijing Chemical Reagent Co., Beijing, China. Sodium montmorillonite (Na-MMT), with cation exchange capacity (CEC) of 90 meq/100 g and particle size of +325 meshes (<45 μm), was purchased from Zhangjiakou Qinghe Chemical Factory, Hebei, China.

2.2. Modification of Na-MMT

The organophilic montmorillonite (organoclay, termed OMMT) was prepared via ion-exchange reaction using alkylammonium. Na-MMT (30 g) was ion-exchanged with 2C18 (19.32 g) in a 1:1 (weight ratio) ethanol-water mixture (500 ml) at 75 °C for 2 h under agitation. The products were filtered and washed repeatedly with the ethanol–water mixture until no Cl^- was detected in the filtrate by a 0.1 mol/l $AgNO_3$ solution. The products were dried for 8 h at 100 °C in vacuum, ground into powder, and finally sifted through a 200-mesh sieve (maximum diameter of 75 μm).

Protonic montmorillonite, denoted as H-MMT, was prepared as follows. Na-MMT (30 g) was ion-exchanged with NH_4Cl (4.8 g) in the de-ionized water (500 ml) at 30 °C for 3 h under agitation. After filtered and washed with de-ionized water until no Cl^- was detected by 0.1 mol/L $AgNO_3$ solution, the product was dried and ground to get NH_4^+ modified MMT at the same condition as OMMT. The powder was then heated at 300 °C for 5 h, so the acidic sites were generated as the following formula [22]:

$$LS^-NH_4^+ \xrightarrow{\Delta} LS^-H^+ + NH_3 \quad (1)$$

where LS^- stands for the structural blocks of the layered silicate.

2.3. Preparation of the PP/MMT compounds

A twin-screw extruder (SHJ30, L/Φ=23, Nanjing Rubber and Plastics Machinery Plant, China) was used for the preparation of the PP/MMT compounds. The operating temperature of the extruder was maintained at 190, 210, 210, and 200 °C from hopper to die, respectively. The screw speed was maintained at 100 rpm. After cooling in water, the extrudates were pelletized. The compound pellets were dried at 50 °C for 6 h before use. Several PP compounds

Table 1
The PP compounds and their composition

Sample code	PP (wt%)	PP-g-MA (wt%)	Clay type & content		C18 ammonium (wt%)
			Type	(wt%)	
PP	100				
PP/Na-MMT	95		Na-MMT	5	
PP/OMMT	95		OMMT	5	
PP/H-MMT	95		H-MMT	5	
PP/C18	98.8				1.2
PP/PP-g-MA	85	15			
PP/PP-g-MA/OMMT	80	15	OMMT	5	

were prepared and their compositions are listed in Table 1. In the PP/C18 blend, the C18 content is 1.2 wt%, equivalent to the molar fraction of 2C18 in the PP/OMMT microcomposite. The thin films of ca. 50 μm in thickness were prepared by compression-molding the pellets of the PP compounds at 200 °C with a pressure of 75 kgf/cm^2 (7.35 MPa).

2.4. Morphological characterization

X-ray diffraction (XRD) patterns were obtained using a Rigaku (Japan) D/max 2400 diffractometer with Cu Kα radiation ($\lambda = 0.154$ nm, 40 kV, 120 mA) at room temperature. The diffractograms were scanned from 1.5° to 40° (2θ) in steps of 0.02° using a scanning rate of 8°/min.

The morphology structures of the composites were investigated by a Hitachi (Japan) H-800 transmission electron microscope (TEM) with an acceleration voltage of 100 kV. The ultrathin slides were obtained by sectioning the injection-molded samples along a direction perpendicular to the injection.

2.5. Ultraviolet exposure test

Ultraviolet (UV) exposure tests were carried out in a WFH-201-B canned UV exposure instrument (Wenzhou Analytic Apparatus Co., China). The working temperature was controlled at 35 ± 2 °C and the wavelength of radiation was 300 nm. The photo-oxidation rate was followed by measuring carbonyl absorbance through FT-IR per 40 h upon UV exposure, for a period from 0 to 320 h. The FT-IR measurements were performed on a Perkin–Elmer System 2000 infrared spectrum analyzer in the wave-number range of 4000–370 cm^{-1}.

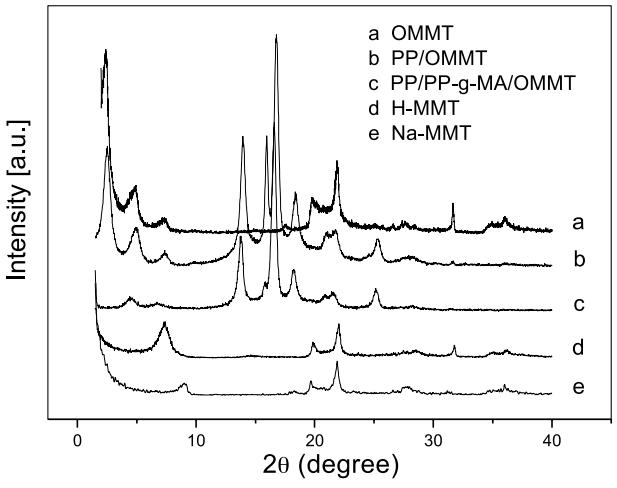

Fig. 1. XRD patterns of Na-MMT, H-MMT, OMMT, PP/OMMT and PP/PP-g-MA/OMMT.

3. Results and discussion

3.1. Characterization of the composites

Fig. 1 shows the X-ray diffraction (XRD) patterns of clays (Na-MMT, H-MMT and OMMT) and composites (PP/OMMT and PP/PP-g-MA/OMMT). Na-MMT and H-MMT display their characteristic peaks at 0.98 and 1.4 nm, respectively, corresponding to the (001) diffraction of layer structure of Na-MMT and H-MMT. OMMT shows a 3.72 nm *d*-spacing. XRD pattern of PP/OMMT composite shows that the silicate dispersed in the polymer matrix retained the stacked structure of the pristine OMMT, with a little decreased layer space (3.56 nm), indicating an immiscible dispersion of the clay in PP matrix. When the compatibilizer PP-g-MA is introduced, the characteristic peak of OMMT disappears in the resultant PP/PP-g-MA/OMMT composite. The absence of the (001) peak in the XRD pattern suggests that the clay has a nearly exfoliated dispersion in the polymer matrix; this is to say, The PP/PP-g-MA/OMMT composite is an exfoliated nanocomposite. The XRD patterns of PP/Na-MMT and PP/H-MMT (not shown in Fig. 1) do not reveal any peak shift in comparison to the corresponding clays, suggesting that they are all of microcomposites.

The TEM images of PP/Na-MMT, PP/H-MMT, PP/OMMT and PP/PP-g-MA/OMMT composites are shown in Fig. 2. Large and unevenly dispersed primary clay particles were observed in PP/Na-MMT composite (Fig. 2(A)), with particle size of 1–1.5 μm. It indicates that the melt processing was able to dissociate the initial clay agglomerates (up to 75 μm in particle dimension) to the

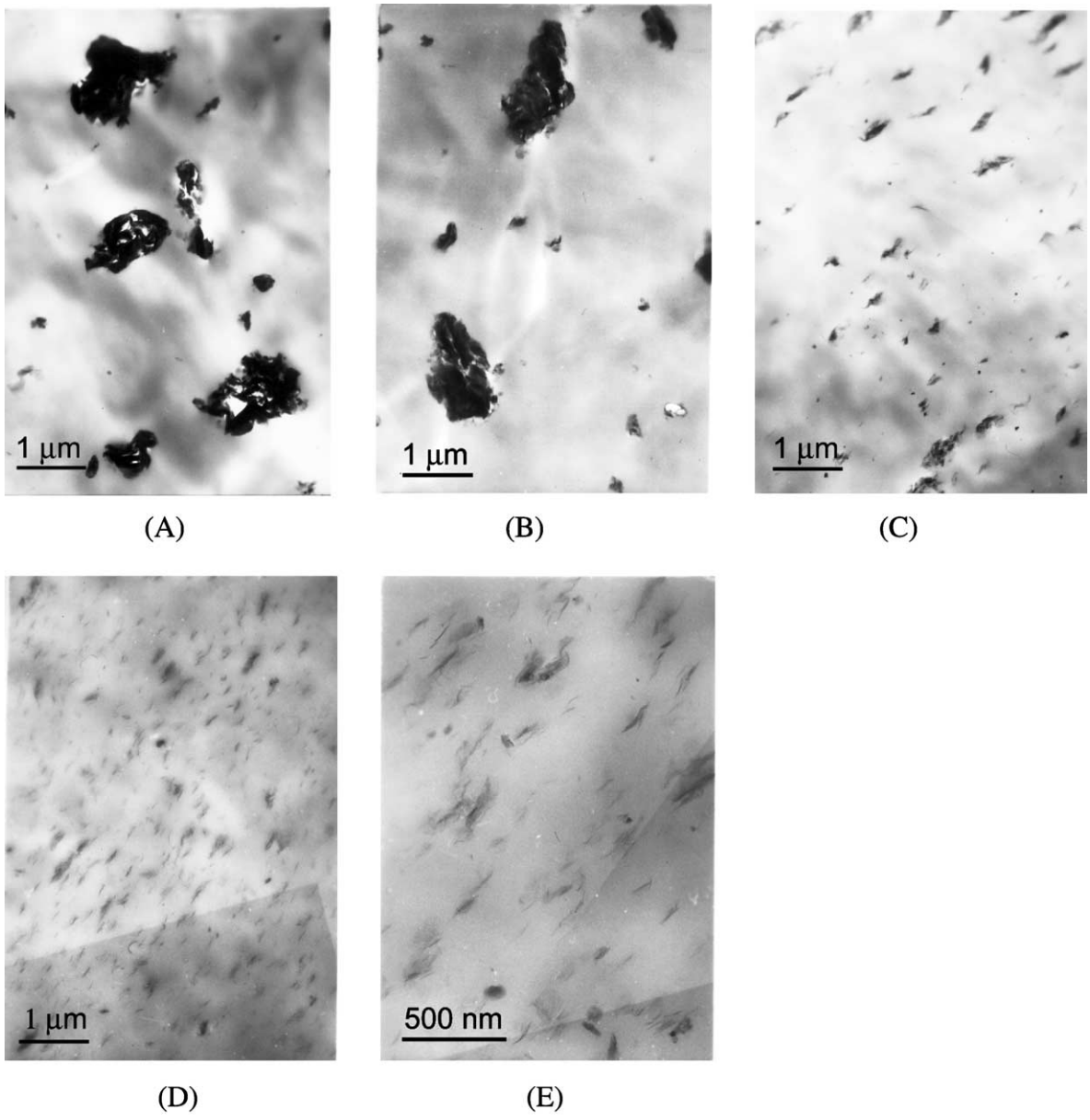

Fig. 2. TEM images of (A) PP/Na-MMT, (B) PP/H-MMT, (C) PP/OMMT, (D) PP/PP-g-MA/OMMT at low magnification and (E) PP/PP-g-MA/OMMT at high magnification.

primary clay particles (<2 μm). The dispersion state of PP/H-MMT composite (Fig. 2(B)) is similar to that of PP/Na-MMT composite, strongly suggesting an immiscible dispersion. On contrary, the submicron particles composed of the silicate aggregates can be observed in PP/OMMT composite (Fig. 2(C)). The particle size is about 0.2–0.5 μm and the polymer matrix is filled homogeneously. Although the initial size of the organoclay is larger than that of the inorganic clay, the organic modification is propitious to the dissociation of the clay particles, resulting in a homogeneous dispersion of silicate layers in the polymer matrix. According to Manias et al., this PP/2C18-MMT composite possesses an immiscible/intercalated structure [19].

The TEM images (Fig. 2(D) and (E)) confirm the partially exfoliated dispersion of the clay in the PP/PP-g-MA/OMMT nanocomposite. The low magnification (Fig. 2(D)) shows the clay is well dispersed throughout the polymer matrix. As seen in the high magnification (Fig. 2(E)), exfoliated clay layers and a few intercalated tactoids are present. Compared the TEM images of PP/PP-g-MA/OMMT nanocomposite and PP/OMMT microcomposite, the addition of PP-g-MA copolymer could promote the dissociation and exfoliated dispersion of the clay particles.

3.2. Infrared analysis

The degradation behavior of organic polymers by UV irradiation is of considerable importance [23]. Under UV

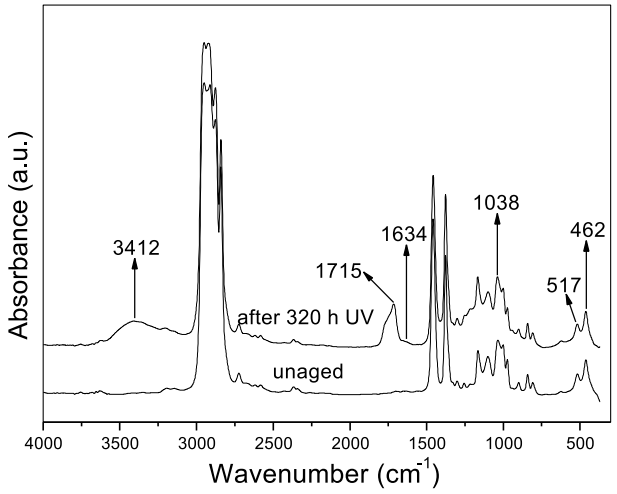

Fig. 3. FT-IR spectra of PP/PP-g-MA/OMMT nanocomposite before and after 320 h UV irradiation.

irradiation, the initial reaction of the decomposition is the formation of alkyl radicals from polymer macromolecules. The propagation step is the formation of hydroperoxides, which can decompose to produce alkoxy radicals. Then the alkoxy radicals abstract hydrogen on the polymeric backbone or undergo a β-scission. At last, different carbonyl species are formed and the polymer matrix suffer degradation.

Infrared spectrometry is a powerful tool for studying the oxidative degradation of polypropylene and more generally of synthetic polymers [24]. Fig. 3 shows the FT-IR spectra of PP/PP-g-MA/OMMT nanocomposite before and after 320 h UV irradiation. The absorption at 1038 cm^{-1} is assigned to Si–O stretching (ν_{Si-O}) of MMT. The bands at 517 and 462 cm^{-1} are assigned to Al–O stretching (ν_{Al-O}) and Si–O bending (δ_{Si-O}) of MMT. In spite of the presence of the compatibilizer, PP-g-MA that contains anhydride groups, there are no absorption bands at 1712 cm^{-1} (carboxylic acid), 1780 and 1850 cm^{-1} (anhydride)

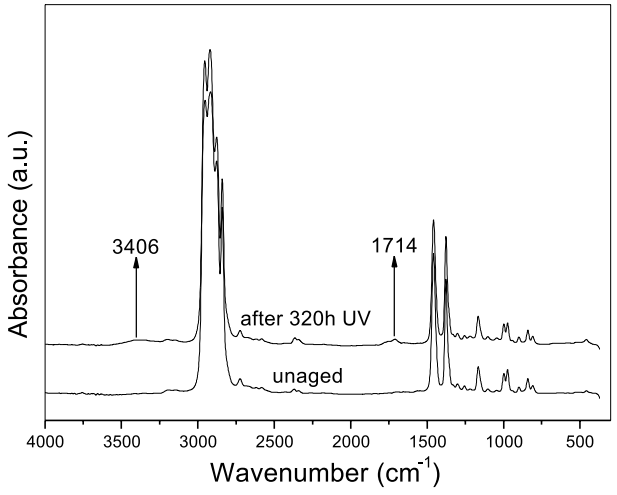

Fig. 4. FT-IR spectra of pure PP before and after 320 h UV irradiation.

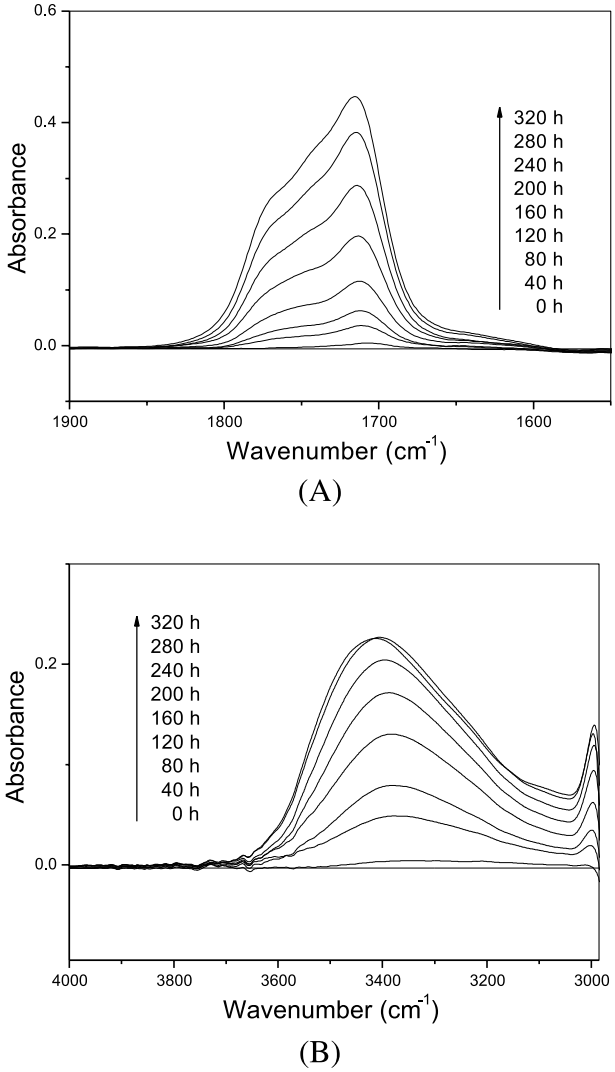

Fig. 5. Evolution of the infrared spectra at different times upon UV irradiation of PP/PP-g-MA/OMMT nanocomposite: (A) in the domain 1900–1550 cm^{-1}; (B) in the domain 4000–3000 cm^{-1}.

observed before UV irradiation. It suggests that the content of anhydride groups is too low to present in the spectrum (considering that the content of PP-g-MA in the nanocomposite is 15% and that the degree of maleation is 0.8%). As shown in the figure, a new broad band appears at about 1715 cm^{-1} after 320 h UV irradiation that belongs to a mixture of different carbonyl species [25]. The second new band at 1634 cm^{-1} shows the resultant of the olefinic band. The third new band at 3412 cm^{-1} belongs to hydroxyl group, which indicates the resultant of hydroperoxides.

Fig. 4 shows the FT-IR spectra of pure PP before and after 320 h UV irradiation. After 320 h UV exposure, the appearance of new bands are similar to those of PP/PP-g-MA/OMMT nanocomposite, but the intensity of these bands of PP is quite far lower than those of PP/PP-g-MA/OMMT nanocomposite.

For the analysis of the photo-oxidative degradation, two domains of the infrared spectrum are of interests,

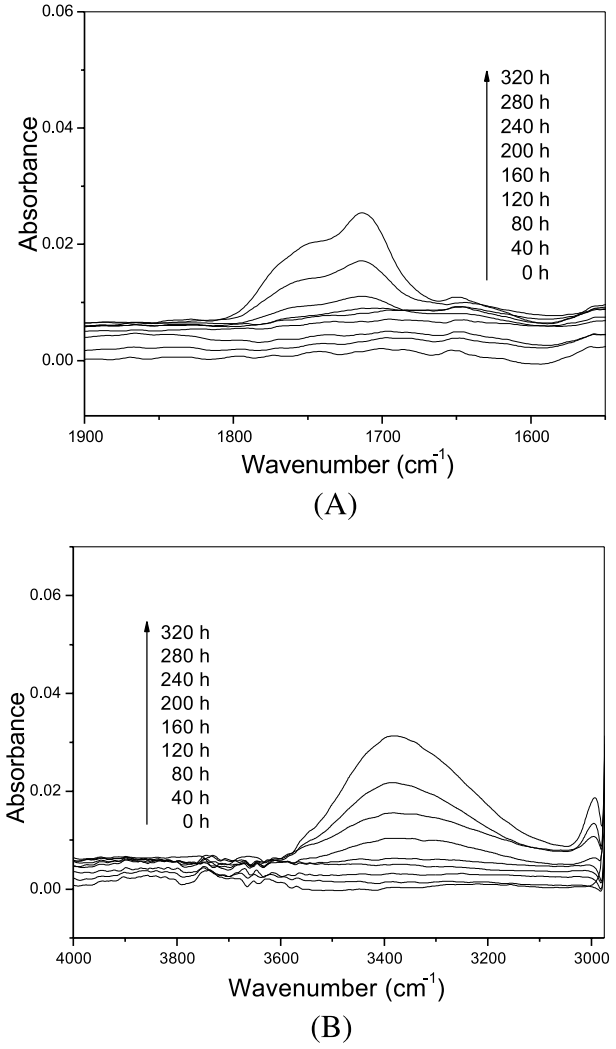

Fig. 6. Evolution of the infrared spectra at different times upon UV irradiation of pure PP: (A) in the domain 1900–1550 cm^{-1}; (B) in the domain 4000–3000 cm^{-1}.

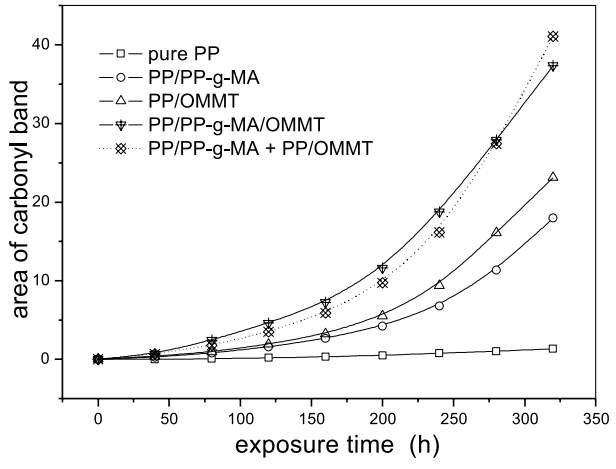

Fig. 7. Variations in the area of carbonyl band during the photo-oxidation of thin films of pure PP, PP/PP-g-MA compound, PP/OMMT microcomposite and PP/PP-g-MA/OMMT nanocomposite.

corresponding to the stretching vibrations of carbonyl (C=O) and hydroxyl (O–H) groups. The film samples were measured by FT-IR per 40 h upon UV exposure for a total irradiation time up to 320 h. Fig. 5 shows the evolution of the infrared spectra of PP/PP-g-MA/OMMT nanocomposite in the carbonyl and hydroxyl regions upon UV irradiation. All spectra were obtained by spectral subtraction of the spectrum of the unirradiated film. It can be seen that with increasing the exposure time, the intensity of the carbonyl and hydroxyl bands grows. This behavior indicates that the material suffers degradation. In the carbonyl region (Fig. 5(A)), the shape of the band suggests that more than one functional group is formed. It could be seen that there are several functional groups peaking at 1715, 1735 and 1780 cm^{-1}. The photoproducts corresponding to these functional groups have been identified previously [25]. The main adsorption at 1715 cm^{-1} belongs to the carbonyl group of carboxylic acids in the dimmer form. The shoulder on the carbonyl band at 1780 cm^{-1} results from the formation of γ-lactones. The attribution of the functional group at 1735 cm^{-1} is postulated to result either from the carbonyl groups of esters or from the carbonyl vibration of carboxylic acids associated to hydroxyl groups. In the hydroxyl region (Fig. 5(B)), the broad band peaking up at 3412 cm^{-1} is composed of the O–H stretching of hydroperoxides and alcohols, with a poor contribution of the O–H adsorption of carboxylic acids.

Fig. 6 shows the evolution of the infrared absorbance of pure PP in the carbonyl and hydroxyl regions upon UV irradiation. It could be seen that the spectra had little change until 120 h. The intensity of the carbonyl and hydroxyl bands grows slower in comparison with the PP/PP-g-MA/OMMT nanocomposite.

The other samples show similar FT-IR spectra upon UV irradiation. The intensity of the carbonyl and hydroxyl bands of all compound samples grows faster than that of pure PP. However, the shape of the oxidation bands is similar to that observed for pure PP. It is suggested that the addition of clays and PP-g-MA does not modified the mechanism of photo-oxidation of the PP matrix.

3.3. The influence of organoclay and compatibilizer on photo-oxidation

Since the presence of compatibilizer does not overlap the carbonyl region of products of the PP oxidation, the area of carbonyl band of FT-IR spectrum of each specimen can be obtained separately and considered as the quantity of the carbonyl [26]. It is the measure of photo-oxidative degradation of the samples. Fig. 7 shows the area of carbonyl band in function of the exposure time for the thin-film samples of pure PP, PP/PP-g-MA compound, PP/OMMT microcomposite and PP/PP-g-MA/OMMT nanocomposite. As shown in the figure, the rate of photo-oxidation of PP/PP-g-MA/OMMT nanocomposite was faster than that of pure PP. The influence of organoclay

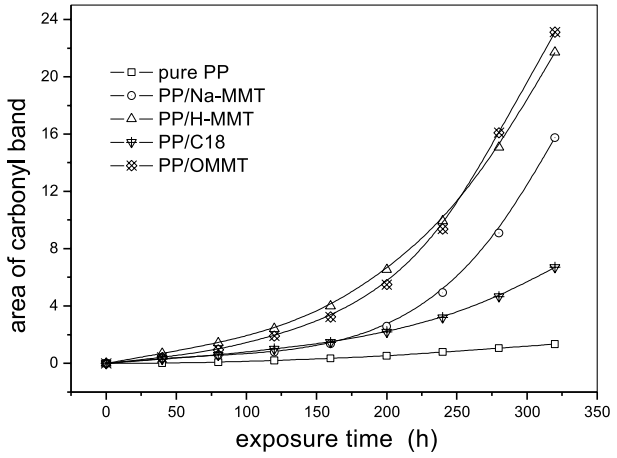

Fig. 8. Variations in the area of carbonyl band during the photo-oxidation of thin films of pure PP, PP/C18 compound and PP/Na-MMT, PP/H-MMT, PP/OMMT microcomposite.

and compatibilizer was reviewed separately by measuring the photo-oxidation of PP/PP-g-MA compound and PP/OMMT microcomposite. The rates of photo-oxidation of PP/PP-g-MA compound and PP/OMMT microcomposite were also faster than that of pure PP. It is indicated that the presence of both PP-g-MA and OMMT can accelerate the photo-oxidation of PP matrix, respectively.

We added the area of carbonyl band of PP/PP-g-MA blend to that of PP/OMMT microcomposite against the UV irradiation time and the results are plotted in Fig. 7. It could be observed that the summation (dot-line) is well consistent to the curve of PP/PP-g-MA/OMMT nanocomposite. Compared the TEM images of PP/OMMT microcomposite (Fig. 2(C)) and of PP/PP-g-MA/OMMT nanocomposite (Fig. 2(D)), it is shown that OMMT can be further intercalated by the polypropylene macromolecules and lead to the formation of a nanocomposite by the addition of PP-g-MA. On contrary, OMMT cannot be further intercalated by the polymer chains and thus form the microcomposite without PP-g-MA. Although the dispersion state of MMT is different (nano- vs. micro-), the rate of photo-oxidation of PP/OMMT microcomposite (with micrometric dispersion of the clay aggregates) is similar to that of PP/PP-g-MA/OMMT nanocomposite (with nanometric dispersion of the clay layers) if pulsing the influence of PP-g-MA. It indicates that the dispersion state of the clay particles in the polymer matrices has a little influence on the photo-oxidative degradation of polymer matrix.

3.4. The influence of MMT and alkylammonium on photo-oxidation

In order to understand the influence of organoclay, we investigated the effect of MMT and alkylammonium on photo-oxidation separately. Fig. 8 shows the area of carbonyl band in function of the exposure time for thin films of pure PP, PP/C18 compound and PP/Na-MMT, PP/H-MMT, PP/OMMT microcomposite. The rates of photo-oxidation of PP/Na-MMT microcomposite and PP/C18 compound are faster than that of pure PP. That is to say, the acceleration of photo-oxidation of PP/OMMT is due to the effects of pristine clay and alkylammonium, in which the effect of pristine clay is primary. It has been reported [27] that the complex crystallographic structure and habit of clay minerals result in some catalytic active sites, such as Bronsted acidic sites like the weakly acidic SiOH and strongly acidic bridging hydroxyl groups at the layer edge of the silicate, un-exchangeable transition metal ions in the galleries, and crystallographic defect sites within the layers. All these active sites can accept single electrons from donor molecules and form free radical, leading to the oxidation of the polymer matrix. As reported in the previous work [14], the transition metal ions in the galleries of MMT can accelerate the photo-oxidation of polyethylene considerably.

The photo-oxidation rate of PP/H-MMT microcomposite is much faster than that of pure PP. Although the dispersion state of the clay in PP/H-MMT is similar to that in PP/Na-MMT, the photo-oxidation of PP/H-MMT is also much faster than that of PP/Na-MMT. It indicates that the acidic sites on the layered silicates can accelerate the photo-oxidative degradation of polymer matrix. These acidic sites can accept single electrons from donor molecules with low ionization potential [27], leading to the formation of free radical upon UV irradiation.

The thermal decomposition of alkyl ammonium salts in the clay interlayer is known to take place following the Hoffman mechanism. The resultant is ammonia, corresponding olefin and an acidic site on layered silicate [28]:

$$\mathrm{LS}^{-+}[\mathrm{NH_3-CH_2-(CH_2)_n-CH_3}] \xrightarrow{\Delta} \mathrm{LS^-H^+ + NH_3 + CH_2=CH-(CH_2)_{n-1}-CH_3} \quad (2)$$

During the melt processing and UV exposure period, the decomposition of the ammonium ions in the galleries happened partially. The decay products, such as the acidic sites and corresponding olefin, can both lead to the formation of free radical and accelerate the photo-oxidative degradation of polymer matrix upon UV irradiation.

4. Conclusions

In the present work, PP/MMT nanocomposite was prepared using the compatibilizer PP-g-MA through melt processing. The photo-oxidative behavior of the PP clay nanocomposite has been investigated upon ultraviolet exposure. The rate of photo-oxidative degradation of PP/MMT nanocomposite is much faster than that of pure PP. The influence of pristine MMT, alkylammonium and compatibilizer were investigated, respectively. All these

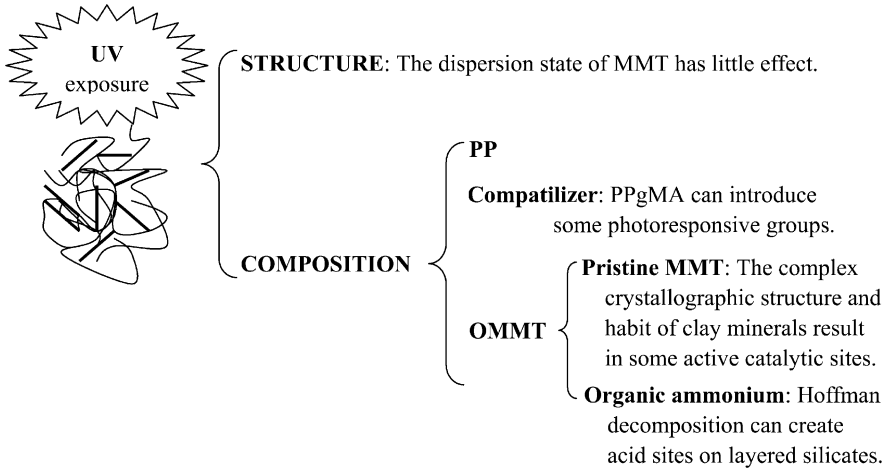

Fig. 9. Schematic representation of catalysis mechanism of photo-oxidative degradation of PP clay nanocomposite.

components can catalyze the photo-oxidation of PP matrix. Moreover, the dispersion state of the clay particles in the polymer matrices has a little influence on the photo-oxidative degradation of polymer matrix. That is to say, the acceleration of photo-oxidative degradation of PP clay nanocomposite is due to the influence of compatibilizer, pristine MMT and interlayer ammonium ions, in which the influence of compatibilizer and pristine MMT is primary.

The compatibilizer, PP-g-MA, can introduce some photoresponsive groups to PP matrix, such as carboxylic acid and anhydride. The complex crystallographic structure and habit of clay minerals result in some catalytic active sites. The decomposition of ammonium ions can lead to catalytic acidic sites created on the layers and correspondingly olefin generated. All these photoresponsive groups and catalytic active sites can accept single electrons from donor molecules of PP matrix with low ionization potential. Under UV exposure, free radicals formed in the polymer matrix and the materials suffered photo-oxidative degradation. Consequently, an integrated catalysis mechanism of the photo-oxidative degradation of PP clay nanocomposite is proposed, as schematically shown in Fig. 9. It would provide benefit direction for the preparation and usage of PLSN.

Acknowledgement

This work was financially supported by the National Natural Science Foundation of China (Grant No. 50473054) and the Major Basic Research Projects of China (Grant No. 2003CB615600).

References

[1] Okada A, Kawasumi M, Kurauchi T, Kamigaito O. Polym Prepr 1987; 28:447.
[2] Giannelis EP. Adv Mater 1996;8:29.
[3] Garces JM, Moll DJ, Bicerano J, Fibiger R, Mcleod DG. Adv Mater 2000;12:1835.
[4] Ray SS, Okamoto M. Prog Polym Sci 2003;28:1539.
[5] Kojima Y, Usuki A, Kawasumi M, Okada A, Fukushima Y, Kurauchi T, et al. J Mater Res 1993;8:1185.
[6] Hotta S, Paul DR. Polymer 2004;45:7639.
[7] Galgali G, Agarwal S, Lele A. Polymer 2004;45:6059.
[8] Zanetti M, Costa L. Polymer 2004;45:4367.
[9] Gopakumar TG, Lee JA, Kontopoulou M, Parent JS. Polymer 2002; 43:5483.
[10] Qin HL, Su QS, Zhang SM, Zhao B, Yang MS. Polymer 2003;44: 7533.
[11] Gilman JW. Appl Clay Sci 1999;15:31.
[12] Alexandre M, Dubios P. Mater Sci Eng 2000;28:3.
[13] Qin HL, Zhao CG, Zhang SM, Chen GM, Yang MS. Polym Degrad Stab 2003;81:497.
[14] Qin HL, Zhang ZG, Feng M, Gong FL, Zhang SM, Yang MS. J Polym Sci, Part B: Polym Phys 2004;42:3006.
[15] Qin HL, Zhang SM, Yang MS, Shen DY. Chem J Chin Univ 2004;25: 197.
[16] Tidjani A, Wilkie CA. Polym Degrad Stab 2001;74:33.
[17] Morlat S, Mailhot B, Gonzalez D, Gardette JL. Chem Mater 2004;16: 377.
[18] Kawasumi M, Hasegawa N, Kato M, Usuki A, Okada A. Macromolecules 1997;30:6333.
[19] Manias E, Touny A, Wu L, Strawhecker K, Lu B, Chung TC. Chem Mater 2001;13:3516.
[20] Morgan AB, Harris JD. Polymer 2003;44:2313.
[21] Reichert P, Nitz H, Klinke S, Brandsch R, Thomann R, Mulhaupt R. Macromol Mater Eng 2000;275:8.
[22] Garcia H, Roth HD. Chem Rev 2002;102:3951.
[23] Joseph PV, Rabello MS, Mattoso LHC, Joseph K, Thomas S. Comp Sci Technol 2002;62:1357.
[24] Rabek JF. Photodegradation of polymers: physical characteristics and applications. Berlin: Springer; 1996.
[25] Philippart JL, Sinturel C, Arnaud R, Gardette JL. Polym Degrad Stab 1999;64:213.
[26] Shen DY. Application of infrared spectra in polymer study. Beijing: Science Press; 1982. p. 105.
[27] Xie W, Gao ZM, Pan WP, Hunter D, Singh A, Vaia R. Chem Mater 2001;13:2980.
[28] Zanetti M, Camino G, Reichert P, Mulhaupt R. Macromol Rapid Commun 2001;22:177.